NANO LETTERS

Letter

pubs.acs.org/NanoLett

Signatures of Cooperative Effects and Transport Mechanisms in Conductance Histograms

Matthew G. Reuter,*[,†,§] Mark C. Hersam,[†,‡] Tamar Seideman,[†] and Mark A. Ratner[†]

[†]Department of Chemistry and [‡]Department of Materials Science and Engineering, Northwestern University, Evanston, Illinois 60208, United States

[§]Computer Science and Mathematics Division and Center for Nanophase Materials Sciences, Oak Ridge National Laboratory, Oak Ridge, Tennessee 37831, United States

Supporting Information

ABSTRACT: We present a computational investigation into the line shapes of peaks in conductance histograms, finding that they possess high information content. In particular, the histogram peak associated with conduction through a single molecule elucidates the electron transport mechanism and is generally well-described by beta distributions. A statistical analysis of the peak corresponding to conduction through two molecules reveals the presence of cooperative effects between the molecules and also provides insight into the underlying conduction channels. This work describes tools for extracting additional interpretations from experimental statistical data, helping us better understand electron transport processes.

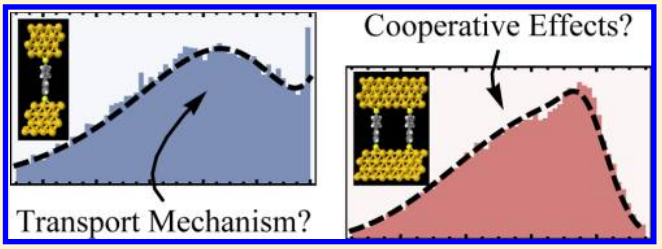

KEYWORDS: *Electron transport, conductance histogram, cooperative effects, transport mechanisms, statistical analysis*

Molecular electronics, the incorporation of molecular components into electrical circuits, has become an active research topic[1] with relevance to catalysis, solar cells, and scanning probe microscopies. Requiring a detailed understanding of charge transfer/transport processes (i.e., how electrons traverse molecules), molecular electronics asks new conceptual questions, most notably,[1−11] "what is the conductance of a single molecular wire connecting two electrodes?" Furthermore, the scaling of such a single-molecule conductance to multiple molecular wires in parallel is also of interest.[2,4,9,12,13]

The key problem in determining a single-molecule conductance is reproducibility.[2−7,9,14−24] Both experimental and theoretical studies have exposed the sensitivity of conductance to changes in the molecule−electrode interface(s),[4−10,14−16,21,22,25−28] and many binding motifs (for example, gold−thiol bonds) exhibit indiscriminate adsorption chemistries.[9,10,21,29,30] Even though progress has been made toward the simultaneous determination of conductance and molecular geometry using, for example, Raman spectroscopy,[31,32] we are generally unable to determine, let alone control, the microscopic geometric details necessary for a well-characterized single-molecule conductance.

This irreproducibility is familiar from studies of quantum point contacts (where groups of metal atoms, instead of molecules, bridge the electrodes),[33−36] and statistical analyses developed for characterizing quantum point contacts have been applied to molecular wires.[2−4,6−10,14,16,17,19,20,22,23,27,28,37] Essentially, conductance measurements from many molecular wire junctions (enough to get reliable statistics, typically thousands or more) are compiled into a conductance histogram (the number of times a conductance G is measured versus G), which reports, abstractly, the probability density function[38] for measuring a particular conductance. Example conductance histograms are shown in Figure 1.

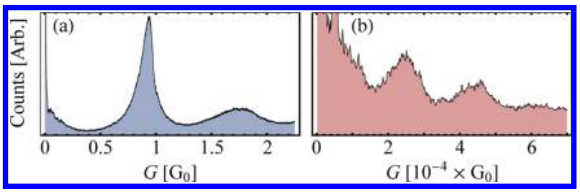

Figure 1. Sample conductance histograms from previous experimental studies. (a) Transport through gold quantum point contacts. (b) Transport through octanedithiol molecules; the peaks at (2.5 and 4.6) × 10^{-4} G_0 correspond to transport through one and two molecules, respectively. The data in panels a and b are from refs 28 and 7, respectively, and are used with permission.

The features in a conductance histogram have, to date, been interpreted in several ways. First, the mean (or mode) of the first peak is attributed to the single-molecule conductance.[2−8,15,17,18,22,23] Second, the width of this peak (its variance) is related to the adsorption chemistry of the molecule with the electrodes[14−16,18,19,23,26,39−42] and is thus indicative of numerous experimental factors. Third, recognizing that electron

Received: December 12, 2011
Revised: March 19, 2012

   dx.doi.org/10.1021/nl204379j | *Nano Lett.* XXXX, XXX, XXX−XXX

transport through molecules is usually a tunneling process (that is, the conductance can vary exponentially with the molecule–electrode geometry), the shape of this peak is often well-described by a log-normal distribution.[14,21,22,24,30,40,43,44] We note, though, that both Gaussian[6,9,15,36,41] and Lorentzian[17,28,41] line shapes have also been used and can, empirically, provide reasonable fits. Lastly, the means/modes of the second and third peaks, if present, are the combined conductances through two and three molecules, respectively.[2,3,7,9,10,15,30] These multiple-molecule peaks tend to appear at (or near) integer multiples of the one-molecule peak.

In this work, we further explore the line shapes of conductance histogram peaks, showing that, similar to conventional spectroscopies (e.g., UV/vis or NMR), these line shapes contain a substantial amount of information. Specifically, we find that the electron transport mechanism (resonant or nonresonant tunneling) is discernible from the one-molecule peak. Each of these mechanisms has a characteristic line shape that is well-described by a beta distribution,[45,46] and one-molecule peaks are generally captured by the sum of these two beta distributions (although the log-normal distribution provides a good fit in specific cases). Additionally, the line shape of the two-molecule peak indicates the presence of cooperative effects between the molecules and also partially reveals the underlying conduction channels[47] through the molecules. After briefly introducing our general (but simple) model and the relevant aspects of electron transport theory, we proceed to demonstrate these assertions.

Conductances are calculated within the Landauer–Imry (coherent scattering) formalism.[48] At zero temperature, the zero-bias conductance is

$$G = G_0 T(E_F) \quad (1)$$

where $G_0 \equiv 2e^2/h$ is the conductance quantum, $T(E)$ is the summed transmission through all conduction channels, and E_F is the electrodes' Fermi level. We use a tight-binding model of the molecular wire junction to obtain $T(E)$, where each molecule contributes a single state/conduction channel (presumably the highest-occupied or lowest-unoccupied molecular orbital) and connects to two semi-infinite electrodes.[12,13,49] Although this model is simple, it qualitatively captures the fundamentals of electron transport and produces exact solutions,[13] thereby facilitating the large number of "measurements" needed to construct conductance histograms. For clarity, the full details of our model are relegated to the Supporting Information; here we note the model's three key parameters, (i) the energy level of each molecular wire, (ii) the electrode-wire coupling, and (iii) the interwire coupling. Finally, we simulate conductance histograms by randomly choosing, for each conductance measurement, these three parameters from Gaussian distributions. The mean values of these parameters are chosen to be representative of realistic systems, following the extensive discussion in section 5 of ref 12. The standard deviations are more arbitrary because they correspond to variations in both the molecular geometry and the adsorption chemistry, which is influenced by, for example, the stability/selectivity of the binding motif and temperature. We assign smaller standard deviations to the wire site energies and the molecule–electrode couplings (these depend mostly on the adsorption chemistry); the interwire coupling also depends on the relative geometries of the two wires and thus receives a larger standard deviation. Table 1 lists the means and standard deviations used throughout the ensuing discussion.

Table 1. Model Parameters Used to Simulate the Conductance Histograms in Figures 2–4[a]

model parameter	mean (eV)	std. dev. (eV)
wire site energy	1.0	0.03
wire-electrode coupling	−0.6	0.0375
interwire coupling	−0.1	0.075

[a]For each individual conductance "measurement," the parameters are chosen from Gaussian distributions with these means and standard deviations.

One-Molecule Junctions. Let us first examine the line shapes of one-molecule peaks. Figure 2a shows the transmission spectrum for a molecular wire junction with the mean parameters listed in Table 1. The spectrum is representative of coherent transport through a single wire/channel; the line shape is mostly Lorentzian with deviations induced by the wire-electrode coupling. Should the Fermi level be near the spectrum's maximum (the resonance, highlighted in blue), the sole conduction channel is completely open, and electron transport occurs by resonant tunneling. Conductances

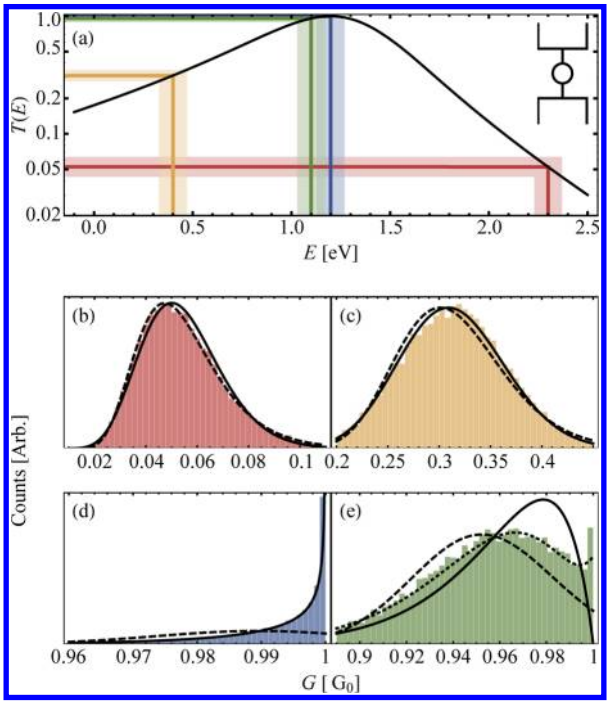

Figure 2. (a) Transmission spectrum through a single wire using the average parameters in Table 1. The red, yellow, green, and blue shadings indicate regimes where transport is far off resonance, off resonance, near resonance, and on resonance, respectively. The shadings' widths depict uncertainty in the molecular geometry, which produces a range of observed conductances (transmissions) for each "measurement." The other panels show simulated conductance histograms for transport (b) far off resonance, (c) off resonance, (d) at resonance, and (e) near resonance, along with proposed line shapes. Each histogram is independently normalized. The dashed lines are the best-fit log-normal distributions (eq 2), the solid lines are the best-fit beta distributions (eq 3), and, for panel e, the short dashed line is the best-fit "double-beta" distribution (eq 4). Whereas the log-normal distribution is excellent for off resonant transport, it fails at or near resonance. The (double-)beta distribution adequately describes all peaks. As discussed in the text, the skewness of the peak is related to the transport mechanism.

dx.doi.org/10.1021/nl204379j | Nano Lett. XXXX, XXX, XXX–XXX

approach G_0 in this case, although we note that inelastic effects (absent from our model) may reduce the molecular conductance.[50,51] Such resonant tunneling is commonly observed in quantum point contacts; see Figure 1a. At Fermi levels away from this resonance (red or yellow), transport occurs by nonresonant tunneling, and conductances are much smaller than G_0. This case is typically reported in transport through molecules (Figure 1b). Lastly is the case of *near* resonant tunneling (green), which has recently been observed in molecular junctions with direct Au−C bonds.[28]

Figure 2b−e displays our simulated conductance histograms for these four cases. We used 25 000 conductance "measurements" to construct each histogram, and each histogram is independently normalized (resulting in the arbitrarily scaled ordinate axes). To develop a theory for these line shapes, we consider the measured conductance through the single channel to be a continuous random variable ($\mathcal{G}_1$) with probability density function $\hat{\mathcal{G}}_1$.

We begin with the off resonance cases in panels b and c. The dashed lines display the best-fit log-normal distributions, $\hat{\mathcal{G}}_1(G) = \hat{\mathcal{L}}(G/G_0;\mu,\sigma^2)$, where

$$\hat{\mathcal{L}}(x;\,\mu,\,\sigma^2) = \frac{1}{x\sqrt{2\pi\sigma^2}}\exp\left[-\frac{(\ln(x)-\mu)^2}{2\sigma^2}\right] \tag{2}$$

is the log-normal distribution.[45] In agreement with previous studies,[14,22,30,40,43,44] these off-resonant histogram peaks are well-described by $\hat{\mathcal{L}}$. The case of resonant transport in panel d, however, exposes the inadequacy of the log-normal distribution for describing conductance histogram peaks. First, the log-normal distribution allows G to be any positive value despite the physical restriction that $0 \le G \le G_0$. In off-resonant cases, $\hat{\mathcal{L}}$ yields a negligible probability of measuring a conductance greater than G_0; however, this is violated at resonance. Moreover, the log-normal distribution has positive skewness[45] (crudely, a peak to the left of a longer right tail), whereas the histogram in panel d is negatively skewed. Gaussian and Lorentzian distributions, which have alternatively been used to describe off-resonant peaks, have similar drawbacks and will also fail to capture the resonant peak.

The beta distribution[38,45,46]

$$\hat{\beta}(x;\,\alpha,\,\beta) = \frac{x^{\alpha-1}(1-x)^{\beta-1}}{B(\alpha,\,\beta)} \tag{3}$$

ameliorates these concerns because it restricts $0 \le x \le 1$ and has flexible skewness. Note that $\alpha > 0$ and $\beta > 0$ in eq 3 are parameters and that $B(\alpha,\beta)$ is the beta function. Supposing that the one-molecule conductance peak is beta-distributed, $\hat{\mathcal{G}}_1(G) = \hat{\beta}(G/G_0;\alpha,\beta)$, the solid lines in Figure 2b−e display the best-fit beta distributions. It is evident that the beta distribution provides a good description of both on- and off-resonant peaks in conductance histograms. Furthermore, the peak line shape is directly tied to the transport mechanism. At resonance, the transmission is capped at 1, and microscopic variations can only decrease the conductance (Figure 2a). Because $G = G_0$ for the average parameters, the histogram peak bunches up at G_0 with a long tail to the left (negative skewness) and has nonzero density at G_0 ($\beta \le 1$ in eq 3). Similarly, histogram peaks for off-resonant transport do not have density at G_0 ($\beta > 1$) and are positively skewed. (From Figure 2a, the transmission spectrum is essentially linear on a semilog scale; that is, fluctuations in the molecular geometry are more likely to increase the conductance.). In this sense, the line shape of a conductance histogram peak reflects the shape of the transmission spectrum near the Fermi level.

As the final case for a one-molecule peak, we consider near resonant transport in Figure 2e. Neither the log-normal nor the beta distribution adequately captures the line shape, as both predict incorrect modes and miss the bump at G_0. In this case, it is likely that the transport is sometimes resonant and sometimes nonresonant, depending on the microscopic details of each individual measurement. To explore this hypothesis, we let $0 \le \gamma \le 1$ be the probability that transport occurs by nonresonant tunneling. Then, the line shape might be described by a "double-beta" distribution that includes contributions from both transport mechanisms

$$\hat{\beta}_2(G/G_0;\,\alpha_1,\,\beta_1,\,\alpha_2,\,\beta_2,\,\gamma) = \gamma\hat{\beta}(G/G_0;\,\alpha_1,\,\beta_1) + (1-\gamma)\hat{\beta}(G/G_0;\,\alpha_2,\,\beta_2) \tag{4}$$

where $\beta_1 > 1$ corresponds to nonresonant transport and $0 < \beta_2 \le 1$ is resonant transport. The short-dashed line in the inset of Figure 2e plots the best-fit double-beta distribution, showing that this distribution captures the peak's line shape. Because the beta distribution is a double-beta distribution with $\gamma = 0$ or 1, the double-beta distribution generally captures the line shape of a one-molecule peak. Table 2 lists the best-fit double-beta parameters for each of these four cases.

Table 2. Best-Fit "Double-Beta" Parameters (eq 4) for Each Histogram Peak in Figure 2

histogram	α_1	β_1	α_2	β_2	γ
2(b)	11.2	195			1
2(c)	25.7	56.4			1
2(d)			55.2	0.537	0
2(e)	54.9	3.24	35.2	1.00	0.701

Therefore, the line shapes of one-molecule peaks in conductance histograms reveal the electron transport mechanism (resonant vs nonresonant tunneling), and, if near resonance, the probability of either mechanism. Although the ability to distinguish resonant from nonresonant tunneling in these line shapes is interesting, we pause to discuss its significance. In principle, the two mechanisms are identifiable from the location of the peak; resonant tunneling will yield a conductance close to G_0, whereas nonresonant tunneling will produce a much smaller conductance. This is easily seen in Figures 1 and 2. The implicit assumption in such an analysis, however, is that only one channel contributes to conduction. Systems with multiple active conduction channels—perhaps quantum point contacts with multivalent metals,[34] molecules with degenerate frontier orbitals,[52,53] or junctions with multiple molecular wires[13]—may have a peak near G_0 without any conduction from resonant tunneling. As we now discuss, such a multiple-channel peak will have a different line shape than that seen in Figures 1a and 2d; that is, the peak line shape corroborates the peak location when identifying the transport mechanism.

Two-Molecule Junctions. Although the generalization to multiple conduction channels from a single channel is mathematically simple—we still use eq 1—multiple channels display much richer physics due to the presence of cooperative effects,[2,4,9,12,13] interferences,[13,54] or both between the channels.

dx.doi.org/10.1021/nl204379j | Nano Lett. XXXX, XXX, XXX−XXX

For this discussion, our two channels will come from two identical molecules in the junction (for simplicity); the other cases listed above, or the presence of additional molecular wires, will not qualitatively change our results. Under these conditions, Figure 3a displays the transmission spectra through

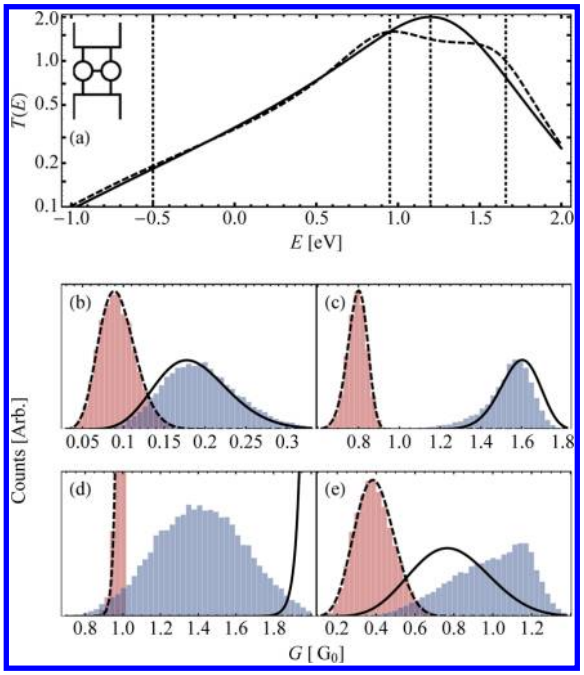

Figure 3. (a) Transmission spectra through two isolated wires (no cooperative effects) and two coupled wires for the average parameters in Table 1 (solid and dashed lines, respectively). Near the isolated molecules' resonances ($E \approx 1.2$ eV), cooperative effects diminish transmission, whereas they *tend* to enhance it away from these resonances.[13] The dotted vertical lines (from left to right) mark the Fermi levels for the conductance histograms displayed in panels b–e, respectively. Each conductance histogram displays the one-molecule peak (red) with its best-fit double-beta distribution (dashed line) along with the simulated two-molecule peak (blue) and the predicted line shape if cooperative effects are ignored (eq 5, solid line). When cooperative effects are small (the two transmission spectra are roughly equal at the Fermi level, panels b and c), the predicted line shapes are reasonable; however, stronger cooperative effects induce noticeable deviations (panels d and e). Each histogram peak is independently normalized.

two isolated wires (no interference or cooperative effects) and two coupled wires, both for the average parameters. Figure 3b–e then shows conductance histograms for the four Fermi levels marked in Figure 3a. Each of these histograms features a one-molecule peak fit with a double-beta distribution as well as the simulated two-molecule peak. As before, we consider the conductance through two molecules to be a random variable ($\mathcal{G}_2$) and interpret the two-molecule peak as the probability density function ($\hat{\mathcal{G}}_2$) for $\mathcal{G}_2$

Without cooperative effects, Ohm's law tells us that the conductance through two molecular wires is twice that through a single wire. Therefore, we expect $\mathcal{G}_2 = 2\mathcal{G}_1$ and[38]

$$\hat{\mathcal{G}}_2(G) = \frac{1}{2}\hat{\mathcal{G}}_1\left(\frac{G}{2}\right) \tag{5}$$

This line shape is also plotted in each of Figure 3's histograms. When cooperative effects are small (i.e., near Fermi levels where the two transmission spectra in Figure 3a are approximately equal), eq 5 adequately describes the two-molecule peak; see panels b and c. Unsurprisingly, cooperative effects can cause significant deviations from this form, as evident in panels d and e.

We recently discussed[13] how cooperative effects shift the underlying conduction channels[47] of the system, a process that ultimately changes the conductance. It is therefore likely that the line shape of a two-molecule peak encodes information on the two conduction channels. For this system, the channels are the "bonding" (in-phase overlap of the molecular levels) and "antibonding" (out-of-phase) channels[13] and are each similar to an isolated channel. In this sense, if we could exclusively measure the conductance through one of these channels, then its histogram should be well-described by a double-beta distribution. Figure 4 verifies that this is indeed the case.

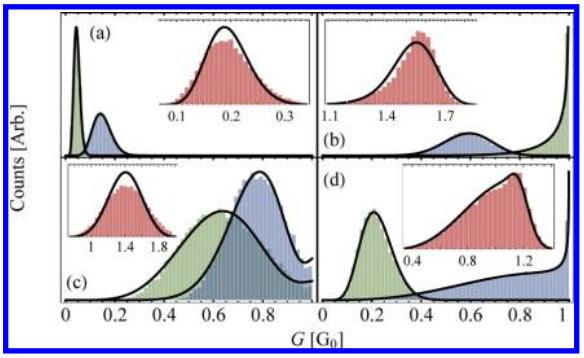

Figure 4. Conductance histograms exploring the relationship between the underlying conduction channels and the line shape of the two-molecule peak. The four panels correspond to those in Figure 3: Figure 4a corresponds to Figure 3b and so on. The main panels show independent histograms for both channels (blue and green) along with each channel's best-fit double-beta line shape. The insets redisplay the two-molecule histograms from Figure 3 along with the line shapes predicted by adding the two channels (eq 6). While slightly inferior to the line shapes presented in Figure 3 when cooperative effects are small, eq 6 adequately predicts the two-molecule line shapes without regard to the magnitude of cooperative effects. The two-molecule line shapes encode information on the underlying conduction channels.

Suppose now that $\mathcal{G}_\pm$ are the random variables for the conductances through the bonding and antibonding channels (with probability density functions $\hat{\mathcal{G}}_\pm$), such that $\mathcal{G}_2 = \mathcal{G}_+ + \mathcal{G}_-$. Then, if $\mathcal{G}_+$ and $\mathcal{G}_-$ are independent random variables (as a first approximation),[55] we find[38]

$$\begin{aligned}\hat{\mathcal{G}}_2(G) &= \int_0^{G_0} \mathrm{d}g_1 \int_0^{G_0} \mathrm{d}g_2 \hat{\mathcal{G}}_+(g_1)\hat{\mathcal{G}}_-(g_2)\delta(G - g_1 - g_2) \\ &= \int_{G_0\max(0,G/G_0-1)}^{G_0\min(1,G/G_0)} \mathrm{d}g \hat{\mathcal{G}}_+(g)\hat{\mathcal{G}}_-(G - g),\end{aligned} \tag{6}$$

where δ is the Dirac delta function. Figure 4 shows that this line shape is reasonably accurate, even when cooperative effects are strong; the discrepancies most likely stem from our assumption that $\mathcal{G}_+$ and $\mathcal{G}_-$ are independent. Furthermore, this $\hat{\mathcal{G}}_2$ is generally not a (double-)beta distribution itself,[46] meaning that multiple-channel peaks near G_0 will have different line shapes than a one-channel peak under resonant tunneling. Regardless of these nuances, Figures 3 and 4 demonstrate that the line

dx.doi.org/10.1021/nl204379j | Nano Lett. XXXX, XXX, XXX–XXX

shape of a two-molecule peak reveals the presence of cooperative effects and contains some information on the underlying conduction channels.

We conclude our discussion by mentioning other factors that might impact our analysis. Experimentally, direct tunneling from one electrode to the other is observed in conductance histograms as a feature that decays as G increases; see the left of Figure 1b. Our model does not include any such contribution, and untangling the actual line shapes of peaks from this background is not always straightforward. Other work has reported systematic methods to aid this process.[15,18,20,23] Furthermore, our model restricts the conductance through a single channel to the range $0 \leq G \leq G_0$, whereas in reality several effects may cause measured conductances to slightly exceed G_0. (See Figure 1a.) Experimental error is one possible culprit, as is the presence of a second, weakly conducting channel for some microscopic geometries. A cross-correlation analysis[37,56] of the raw conductance data may help elucidate this behavior.

Summary. We have examined the line shapes of peaks in conductance histograms, showing that these line shapes, similar to those in conventional spectroscopies, possess high information content. Specifically, the one-molecule peak is well-described by a "double-beta" distribution (eq 4) that incorporates contributions from both resonant and nonresonant tunneling. When *near* resonance, this line shape reflects the relative frequencies of these conduction mechanisms. If, however, only one mechanism contributes to conduction, then the peak will have a distinguishable line shape; *a positive skewness indicates nonresonant tunneling, whereas a negative skewness corresponds to resonant tunneling*. Considering the two-molecule peak, the line shape reveals the presence of cooperative effects (compare the two-molecule peak to "twice" the one-molecule peak, eq 5) and additionally encodes the nature of the underlying conduction channels (to a good approximation, eq 6).

To our knowledge, this work represents the first general analysis of these line shapes, although investigations of one-molecule peaks under nonresonant tunneling conditions have been reported.[14,15] Despite using a simple model due to the availability of exact solutions, we believe our results to be general. For instance, the histogram peaks predicted by our model in Figures 2 and 3 strongly resemble (at least qualitatively) those of the experimental histograms presented in Figure 1. That said, this contribution is just a first step. Additional work to understand the (small) correlation between the underlying conduction channels will enhance our predictions of multiple-channel peaks. Moreover, the inverse problem of inferring the conduction channels from a multiple-molecule peak is far more relevant and will be discussed at a later time. Here we suffice to show that transport mechanisms determine the one-molecule peak and conduction channels dictate multiple-molecule peaks.

■ ASSOCIATED CONTENT

Supporting Information

Full details of our model and of the best-fit distributions in Figures 2–4. This material is available free of charge via the Internet at http://pubs.acs.org/.

■ AUTHOR INFORMATION

Corresponding Author

*E-mail: reutermg@ornl.gov.

Notes

The authors declare no competing financial interest.

■ ACKNOWLEDGMENTS

We thank Gemma Solomon for helpful conversations and Latha Venkataraman and Nongjian Tao (and their groups) for sharing with us the data in Figure 1. M.G.R. performed this research as a Department of Energy (DOE) Computational Science Graduate Fellow (grant no. DE-FG02–97ER25308) while at Northwestern University and as a Eugene P. Wigner Fellow at the Oak Ridge National Laboratory, which is managed by UT-Battelle, LLC, for the U.S. DOE under contract DE-AC05–00OR22725. We further acknowledge support from the NSF (DMR-1121262), MRSEC (DMR-0520513), and the DOE (DE-SC0001785).

■ REFERENCES

(1) Cuevas, J. C.; Scheer, E. *Molecular Electronics*; World Scientific, Hackensack, NJ, 2010.
(2) Xu, B.; Tao, N. J. *Science* **2003**, *301*, 1221–1223.
(3) Mayor, M.; Weber, H. B. *Angew. Chem., Int. Ed.* **2004**, *43*, 2882–2884.
(4) Xiao, X.; Xu, B.; Tao, N. J. *Nano Lett.* **2004**, *4*, 267–271.
(5) Haiss, W.; Nichols, R. J.; van Zalinge, H.; Higgins, S. J.; Bethell, D.; Schiffrin, D. J. *Phys. Chem. Chem. Phys.* **2004**, *6*, 4330–4337.
(6) Venkataraman, L.; Klare, J. E.; Tam, I. W.; Nuckolls, C.; Hybertsen, M. S.; Steigerwald, M. L. *Nano Lett.* **2006**, *6*, 458–462.
(7) Li, X.; He, J.; Hihath, J.; Xu, B.; Lindsay, S. M.; Tao, N. *J. Am. Chem. Soc.* **2006**, *128*, 2135–2141.
(8) Chen, F.; Hihath, J.; Huang, Z.; Li, X.; Tao, N. J. *Annu. Rev. Phys. Chem.* **2007**, *58*, 535.
(9) Li, C.; Pobelov, I.; Wandlowski, T.; Bagrets, A.; Arnold, A.; Evers, F. *J. Am. Chem. Soc.* **2008**, *130*, 318–326.
(10) Nichols, R. J.; Haiss, W.; Higgins, S. J.; Leary, E.; Martín, S.; Bethell, D. *Phys. Chem. Chem. Phys.* **2010**, *12*, 2801–2815.
(11) Leary, E.; González, M. T.; van der Pol, C.; Bryce, M. R.; Filippone, S.; Martin, N.; Rubio-Bollinger, G.; Agraït, N. *Nano Lett.* **2011**, *11*, 2236–2241.
(12) Landau, A.; Kronik, L.; Nitzan, A. *J. Comput. Theor. Nanosci.* **2008**, *5*, 535.
(13) Reuter, M. G.; Solomon, G. C.; Hansen, T.; Seideman, T.; Ratner, M. A. *J. Phys. Chem. Lett.* **2011**, *2*, 1667–1671.
(14) Engelkes, V. B.; Beebe, J. M.; Frisbie, C. D. *J. Phys. Chem. B* **2005**, *109*, 16801–16810.
(15) González, M. T.; Wu, S.; Huber, R.; van der Molen, S. J.; Schönenberger, C.; Calame, M. *Nano Lett.* **2006**, *6*, 2238–2242.
(16) Ulrich, J.; Esrail, D.; Pontius, W.; Venkataraman, L.; Millar, D.; Doerrer, L. H. *J. Phys. Chem. B* **2006**, *110*, 2462–2466.
(17) Venkataraman, L.; Klare, J. E.; Nuckolls, C.; Hybertsen, M. S.; Steigerwald, M. L. *Nature* **2006**, *442*, 904–907.
(18) Jang, S.-Y.; Reddy, P.; Majumdar, A.; Segalman, R. A. *Nano Lett.* **2006**, *6*, 2362–2367.
(19) Quek, S. Y.; Venkataraman, L.; Choi, H. J.; Louie, S. G.; Hybertsen, M. S.; Neaton, J. B. *Nano Lett.* **2007**, *7*, 3477–3482.
(20) Hihath, J.; Tao, N. *Nanotechnology* **2008**, *19*, 265204.
(21) Paulsson, M.; Krag, C.; Frederiksen, T.; Brandbyge, M. *Nano Lett.* **2009**, *9*, 117–121.
(22) Guo, S.; Hihath, J.; Díez-Pérez, I.; Tao, N. *J. Am. Chem. Soc.* **2011**, *133*, 19189–19197.
(23) Gotsmann, B.; Riel, H.; Lörtscher, E. *Phys. Rev. B* **2011**, *84*, 205408.
(24) Reus, W. F.; Nijhuis, C. A.; Barber, J. R.; Thuo, M. M.; Tricard, S.; Whitesides, G. M. *J. Phys. Chem. C* **2012**, *116*, 6714–6733.
(25) Guisinger, N. P.; Greene, M. E.; Basu, R.; Baluch, A. S.; Hersam, M. C. *Nano Lett.* **2004**, *4*, 55–59.

(26) Hines, T.; Diez-Perez, I.; Hihath, J.; Liu, H.; Wang, Z.-S.; Zhao, J.; Zhou, G.; Müllen, K.; Tao, N. *J. Am. Chem. Soc.* **2010**, *132*, 11658−11664.
(27) Cheng, Z.-L.; Skouta, R.; Vazquez, H.; Widawsky, J. R.; Schneebeli, S.; Chen, W.; Hybertsen, M. S.; Breslow, R.; Venkataraman, L. *Nat. Nanotechnol.* **2011**, *6*, 353−357.
(28) Chen, W.; Widawsky, J. R.; Vázquez, H.; Schneebeli, S. T.; Hybertsen, M. S.; Breslow, R.; Venkataraman, L. *J. Am. Chem. Soc.* **2011**, *133*, 17160−17163.
(29) Bilić, A.; Reimers, J. R.; Hush, N. S. *J. Chem. Phys.* **2005**, *122*, 094708.
(30) Haiss, W.; Martín, S.; Leary, E.; van Zalinge, H.; Higgins, S. J.; Bouffier, L.; Nichols, R. J. *J. Phys. Chem. C* **2009**, *113*, 5823−5833.
(31) Ward, D. R.; Halas, N. J.; Ciszek, J. W.; Tour, J. M.; Wu, Y.; Nordlander, P.; Natelson, D. *Nano Lett.* **2008**, *8*, 919−924.
(32) Shamai, T.; Selzer, Y. *Chem. Soc. Rev.* **2011**, *40*, 2293−2305.
(33) Krans, J. M.; van Ruitenbeek, J. M.; Fisun, V. V.; Yanson, I. K.; de Jongh, L. J. *Nature* **1995**, *357*, 767−769.
(34) Yanson, A. I.; van Ruitenbeek, J. M. *Phys. Rev. Lett.* **1997**, *79*, 2157.
(35) Yanson, A. I. Atomic Chains and Electronic Shells: Quantum Mechanisms for the Formation of Nanowires. Ph.D. Thesis, Leiden University, Leiden, The Netherlands, 2001.
(36) Ittah, N.; Yutsis, I.; Selzer, Y. *Nano Lett.* **2008**, *8*, 3922−3927.
(37) Makk, P.; Tomaszewski, D.; Martinek, J.; Balogh, Z.; Csonka, S.; Wawrzyniak, M.; Frei, M.; Venkataraman, L.; Halbritter, A. *ACS Nano* **2012**, DOI: 10.1021/nn300440f.
(38) Ghahramani, S. *Fundamentals of Probability*, 2nd ed.; Prentice-Hall: Upper Saddle River, NJ, 2000.
(39) Lörtscher, E.; Weber, H. B.; Riel, H. *Phys. Rev. Lett.* **2007**, *98*, 176807.
(40) Song, H.; Lee, T.; Choi, N.-J.; Lee, H. *Appl. Phys. Lett.* **2007**, *91*, 253116.
(41) Andrews, D. Q.; van Duyne, R. P.; Ratner, M. A. *Nano Lett.* **2008**, *8*, 1120−1126.
(42) Nagashima, S.; Takahashi, Y.; Kiguchi, M. *Beilstein J. Nanotechnol.* **2011**, *2*, 755−759.
(43) Kim, T.-W.; Wang, G.; Lee, H.; Lee, T. *Nanotechnology* **2007**, *18*, 315204.
(44) Song, H.; Lee, T.; Choi, N.-J.; Lee, H. *J. Vac. Sci. Technol., B* **2008**, *26*, 904−908.
(45) Evans, M.; Hastings, N.; Peacock, B. *Statistical Distributions*, 3rd ed.; Wiley Series in Probability and Statistics; John Wiley & Sons: New York, 2000.
(46) *Handbook of Beta Distribution and Its Applications*; Gupta, A. K., Nadarajah, S., Eds.; Marcel Dekker: New York, 2004.
(47) Paulsson, M.; Brandbyge, M. *Phys. Rev. B* **2007**, *76*, 115117.
(48) Imry, Y.; Landauer, R. *Rev. Mod. Phys.* **1999**, *71*, S306.
(49) Reuter, M. G. *J. Chem. Phys.* **2010**, *133*, 034703.
(50) Galperin, M.; Ratner, M. A.; Nitzan, A. *J. Chem. Phys.* **2004**, *121*, 11965−11979.
(51) Paulsson, M.; Frederiksen, T.; Ueba, H.; Lorente, N.; Brandbyge, M. *Phys. Rev. Lett.* **2008**, *100*, 226604.
(52) Bergfield, J. P.; Barr, J. D.; Stafford, C. A. *ACS Nano* **2011**, *5*, 2707−2714.
(53) Bergfield, J. P.; Barr, J. D.; Stafford, C. A. *Beilstein J. Nanotechnol.* **2012**, *3*, 40−51.
(54) Solomon, G. C.; Andrews, D. Q.; Hansen, T.; Goldsmith, R. H.; Wasielewski, M. R.; van Duyne, R. P.; Ratner, M. A. *J. Chem. Phys.* **2008**, *129*, 054701.
(55) We know these channels are not completely independent. For instance, ref 13 showed that the channels' resonances will still be in the vicinity of the isolated wire's resonance. (See Figure 3a.) Therefore, if we know the bonding channel is near resonance, then the antibonding channel is more likely to be near resonance as well.
(56) Halbritter, A.; Makk, P.; Mackowiak, S.; Csonka, S.; Wawrzyniak, M.; Martinek, J. *Phys. Rev. Lett.* **2010**, *105*, 266805.